Appl. Math. Mech. -Engl. Ed., **36**(1), 37–46 (2015)
DOI 10.1007/s10483-015-1893-9

Applied Mathematics and Mechanics (English Edition)

Effects of microstructure on uniaxial strength asymmetry of open-cell foams*

Zi-xing LU, Ji-xiang HUANG, Ze-shuai YUAN

(Institute of Solid Mechanics, Beihang University, Beijing 100191, P. R. China)

Abstract Based on the elongated Kelvin model, the effect of microstructure on the uniaxial strength asymmetry of open-cell foams is investigated. The results indicate that this asymmetry depends on the relative density, the solid material, the cell morphology, and the strut geometry of open-cell foams. Even though the solid material has the same tensile and compressive strength, the tensile and compressive strength of open-cell foams with asymmetrical sectional struts are still different. In addition, with the increasing degree of anisotropy, the uniaxial strength as well as the strength asymmetry increases in the rise direction but reduces in the transverse direction. Moreover, the plastic collapse ratio between two directions is verified to depend mainly on the cell morphology. The predicted results are compared with Gibson and Ashby's theoretical results as well as the experimental data reported in the literature, which validates that the elongated Kelvin model is accurate in explaining the strength asymmetry presented in realistic open-cell foams.

Key words open-cell foam, microstructure, strength, Kelvin model

Chinese Library Classification O341
2010 Mathematics Subject Classification 74A30, 74A60, 74M25

1 Introduction

Strength is one of the most concerned issues during the design and engineering application of cellular solids. Due to the special construction of open-cell foams, the strength related to those of the solids making up of the foams, to the cell morphology, to the strut geometry, and to the relative density, needs a comprehensive understanding for the successful structural application[1]. The yield strength of open-cell foams under uniaxial and multiaxial loading has been widely investigated. Generally, the plastic collapse stress was obtained by assuming the plastic hinge formation at the nodes. Gibson et al.[2] studied the plastic collapse stress of foams under multiaxial loads theoretically and experimentally. Gioux et al.[3] also investigated the failure problem of the aluminum foams, which had open or closed cells, under biaxial and axisymmetric triaxial loading. Extending the model of open-cell foams to that with doubly tapered struts, Kim and Al-Hassani[4] studied the influence of axial yielding of struts, which were aligned to the applied loading direction, on the plastic yield surface under multiaxial loading conditions, and it was found that the shape of plastic yield surface depended not only

* Received Apr. 14, 2014 / Revised Jun. 3, 2014
Project supported by the National Natural Science Foundation of China (Nos. 11472025 and 11272030)
Corresponding author Zi-xing LU, Professor, Ph. D., E-mail: luzixing@buaa.edu.cn

on the relative density but also on the strut morphology. Based on the experimental results, Amsterdam et al.[5] confirmed that the plastic collapse stress can be predicted by measuring the parameters in an amended equation, where the power-law hardening of the based material was taken into account[6–7].

However, the studies mentioned above ignored the strength asymmetry existing in the realistic open-cell foams. Actually, some materials have different uniaxial tensile and compressive strengths, which may arise as a result of the material failing by different mechanisms in tension and compression. This may also arise in cellular materials due to the different compressive and tensile strengths of the solid material which makes up of the cellular solid, such as trabecular bone and rigid polyurethane foams[8]. Using a simple tetrahedral unit cell, Ford and Gibson[8] predicted the density-dependence and compression-strong strength asymmetry in the open-cell foams when the compression yield strength of the solid material was higher than the tension one and struts were loaded by bending moments and axial forces simultaneously. When investigating the yielding behavior of open-cell foams influenced by strut geometry, Xie and Chan[9] concluded that different compressive and tensile collapse strengths could be exhibited by the open-cell foam which had asymmetrical sectional struts, but the quantitative analysis about the effect of strut geometry on strength asymmetry is lacking. Moreover, a lot of recent experiments on the microstructure of open-cell foams showed that most cells of open-cell foams are somewhat elongated along a certain direction, which resulted from the manufacturing process. By X-ray tomography, Perrot et al.[10] measured the aspect ratio of 1.26–1.56 for open-cell aluminum foams. Jang et al.[11] and Gong et al.[12] investigated the geometric characteristics of a series of open-cell polyester urethane foams, including cell and strut geometry as well as the distribution of the material in the struts and nodes. In conclusion, they found that the anisotropic ratio tested ranged from 1.2 to 1.5 generally.

In recent years, the Kelvin model has been used by a number of groups to study various mechanical and physical properties of open-cell foams. Xie et al.[13] improved the Kelvin model to examine theoretically the elastic properties of the open-cell foam. Thiyagasundaram et al.[14] used a finite element method (FEM) to predict the orthotropic properties of open-cell foams with tetrakaidecahedral unit cells. An anisotropic Kelvin model was developed by Jang et al.[15] to predict the compressive strength of anisotropic, aluminum alloy, open-cell foams. The predictions are generally in very good agreement with the corresponding measurements. Recently, Li et al.[16] used the 3D Kelvin model to investigate the dynamic compressive properties of the open-cell aluminum foam and to analyze qualitatively the effects of the impact velocity and the relative density on the deformation modes, plateau stress, densification strain, and energy absorption of the open-cell foam. In addition, the Kelvin model has been used to investigate the electrical conductivity[17] and the effective thermal conductivity[18] of the foam materials. The author has also used the Kelvin model to investigate theoretically the mechanical behaviour of nanoporous materials influenced by the surface effects[19] and to study the effect of defects on the compressive behavior of open-cell metal foams based on the FEM[20].

Though the microstructure is known to play a decisive role in the mechanical behaviors of open-cell foams, its effect on the strength asymmetry observed in realistic open-cell foams has not been investigated, and such geometric characteristics are essential for quantitatively accurate predictions. In this paper, the effects of the strut geometry and cell morphology on the uniaxial strength asymmetry of open-cell foams are investigated based on the elongated Kelvin model proposed by Lu et al.[21–22]. This modified model has been validated to be effective in predicting the mechanical properties of open-cell foams in previous studies[21–23].

2 Geometrical and mechanical description of model

To describe the actual cell morphology of open-cell foams, the Kelvin model is elongated in one orthogonal direction, always the rise direction due to the foaming and rising process.

Figure 1 shows the elongated Kelvin models loaded in the rise direction and the transverse direction, which contain six quadrilateral faces and eight irregular hexagonal faces. The inclination angle β defines the orientation of the hexagonal faces with respect to the rise direction, and the parameter λ is defined as the anisotropic ratio with $\lambda = \tan\beta$. The initial length of struts in the Kelvin models is denoted by l. According to the periodicity and symmetry of Kelvin models in the whole space, the periodic structural cells simplified from them are illustrated in Fig. 2. These structural cells are restrained by mirror planes ranging from the initial state to the deformed one, which were adopted in the analysis for isotropic open-cell foams[24].

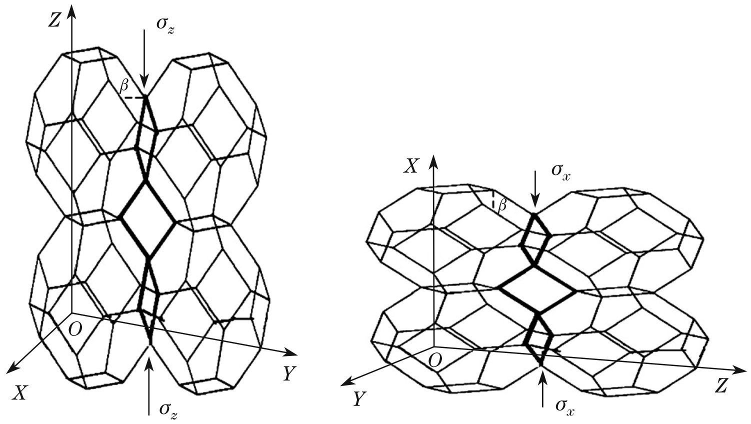

(a) Rise direction (b) Transverse direction

Fig. 1 Elongated Kelvin model loaded in rise and transverse directions

As shown in Fig. 2, the uniaxial compressive forces $2F$ are applied to the structural cells in the rise direction (the Z-direction) and the transverse direction (the X-direction), respectively. The lengths of struts are different in the two different structural cells. In Fig. 2(a), the faces in the XY-plane normal to the rise direction are still square, and the lengths of struts that lie in this plane remain unchanged. Only the lengths of four inclined struts inside the cell change, and the angles between the inclined struts and the XY-plane turn to β. Similarly, in Fig. 2(b), the lengths of inclined struts EC and ED are changed to $\sqrt{\lambda^2+1}l/\sqrt{2}$, while the lengths of inclined struts EA and EB, which lie in the XY-plane that is normal to the rise direction,

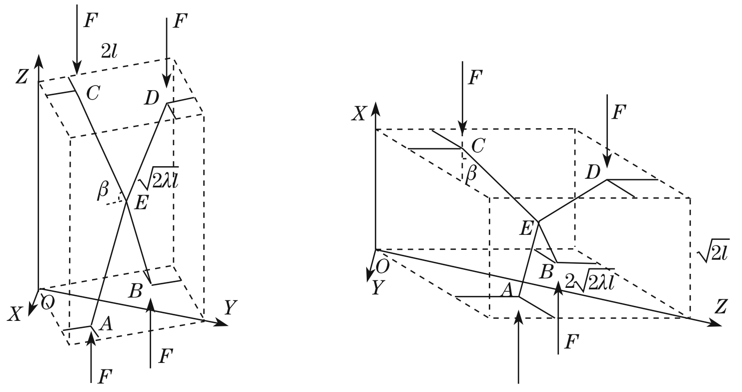

(a) Rise direction (b) Transverse direction

Fig. 2 Periodic structural cell when loaded in rise and transverse directions remain unchanged. The angles between struts (EC, ED) and the X-direction also turn to β, whereas the angles between struts (EA, EB) and the X-direction are still $\pi/4$. What is different from Fig. 2(a) is that the face in the YZ-plane, parallel to the rise direction, changes to a rhombus with the diagonal lengths $2\sqrt{2}\lambda l$ and $2\sqrt{2}l$. Though the geometries of the two cells are different, the same loading situation is still possessed. Only by the four inclined struts transmit the remote force, and the sum of moments in the point E is zero, those struts normal to the loading direction cannot bend, and the diagonal mirror symmetry planes in the structure cell imply that no joint rotates in the cell. It means that only the consideration of the inclined struts is required in this analysis.

The relative density of the anisotropic open-cell foams is then given by the anisotropic ratio λ, the strut cross sectional area S, and the length l, i.e.,

$$\frac{\rho^*}{\rho_{\rm s}} = \frac{\sqrt{2}\sqrt{1+\lambda^2}+1}{2\sqrt{2}\lambda}\frac{S}{l^2}, \tag{1}$$

where ρ^* is the density of the foam materials, and $\rho_{\rm s}$ is the density of the solid materials.

The application of a remote uniaxial force σ_z in the Z-direction (see Fig. 1(a)) produces an axial stress and a bending moment on the inclined strut (see Fig. 3). The maximum moment $M_{\max}$ and the axial stress $\sigma_{\rm a}$ are given by

$$M_{\max} = \frac{1}{2}F\cos\beta\frac{\sqrt{2}l}{2\cos\beta} = \frac{\sqrt{2}Fl}{4}, \tag{2}$$

$$\sigma_{\rm a} = \frac{F\sin\beta}{S}, \tag{3}$$

where F is the vertical force applied to the inclined strut, and the plastic collapse stress in the rise direction of the open-cell foams is $\sigma_{\rm pl}^z = 2F/4l^2$.

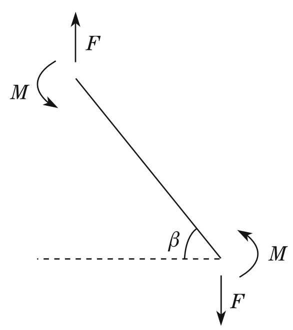

Fig. 3 Application of remote uniaxial stress in Z-direction in Fig. 2(a) produces bending moment M and force F on each inclined strut of cell

The mechanisms of deformation and failure in the transverse direction are the same as that in the rise direction. However, in this case, the maximum moment $M'_{\max}$ in the cell occurs only at the ends of the inclined struts EC and ED, i.e.,

$$M'_{\max} = \frac{1}{2}F\sin\beta\frac{\sqrt{2}l}{2\cos\beta} = \frac{\sqrt{2}Fl}{4}\tan\beta. \tag{4}$$

The corresponding axial stress $\sigma'_{\rm a}$ is given by

$$\sigma'_{\rm a} = \frac{F\cos\beta}{S}, \tag{5}$$

where F is the vertical force applied to the inclined strut with the plastic collapse stress in the transverse direction of the open-cell foams $\sigma_{\rm pl}^{x} = 2F/(4\lambda l^2)$.

As the solid material of foams yields, plastic hinges form near the ends of the inclined struts. Failure occurs when the strut has yielded across its entire section. The total stress distribution across the section of an inclined strut which has failed with the formation of plastic hinge is the sum of bending and axial stress, as shown in Fig. 4. For the square cross section, the width is denoted by $a_{\rm s}$. Therefore, the depth of the neutral axis $\zeta_{\rm s}$ is given by equating forces above and below the neutral axis in Fig. 5, i.e.,

$$\zeta_{\rm s} = a_{\rm s}\Big(\frac{\sigma_{\rm ys}^{\rm c} + \sigma_{\rm a}}{\sigma_{\rm ys}^{\rm c} + \sigma_{\rm ys}^{\rm t}}\Big), \tag{6}$$

where $\sigma_{\rm ys}^{\rm c}$ and $\sigma_{\rm ys}^{\rm t}$ are the compressive and tensile yield strengths of the solid material, respectively. The moment required to cause formation of a plastic hinge is then given by the force $(\sigma_{\rm ys}^{\rm t} - \sigma_{\rm a})a_{\rm s}\zeta_{\rm s}$ times the moment arm $a_{\rm s}/2$, i.e.,

$$M_{\rm p}^{\rm s} = (\sigma_{\rm ys}^{\rm t} - \sigma_{\rm a})\frac{a_{\rm s}^2\zeta_{\rm s}}{2}. \tag{7}$$

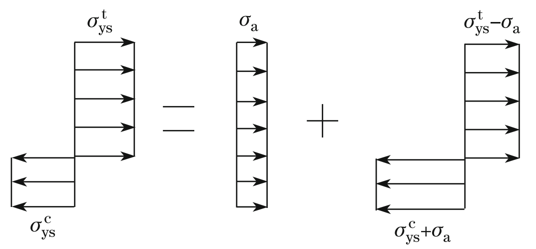

Fig. 4 Bending, axial, and total stress distributions across cross section of inclined strut

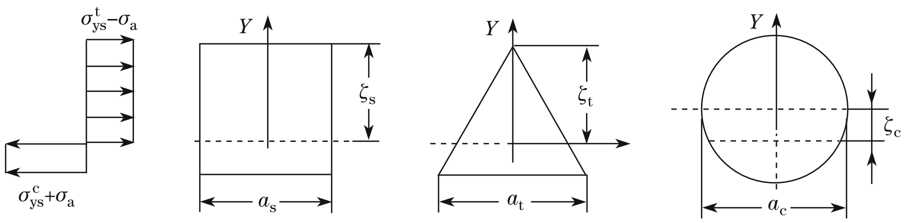

Fig. 5 Bending stress distributions and neutral axes of struts of square, equilateral triangular, and circular cross sections

Substituting (6) into (7) yields

$$M_{\rm p}^{\rm s} = \frac{a_{\rm s}^3}{2}\Big(\frac{\sigma_{\rm ys}^{\rm t}\sigma_{\rm ys}^{\rm c} + (\sigma_{\rm ys}^{\rm t} - \sigma_{\rm ys}^{\rm c})\sigma_{\rm a} - \sigma_{\rm a}^2}{\sigma_{\rm ys}^{\rm t} + \sigma_{\rm ys}^{\rm c}}\Big). \tag{8}$$

By equating the applied maximum moments $M_{\max}$ and $M'_{\max}$ with the plastic moment $M_{\rm p}^{\rm s}$, the equations governing the uniaxial tensile and compressive strengths $\sigma_{\rm pl}^{z}$ and $\sigma_{\rm pl}^{x}$ of the anisotropic open-cell foams can be obtained, respectively,

$$\pm\sqrt{2}\sigma_{\mathrm{pl}}^{z}\Big(\frac{l}{a_{\mathrm{s}}}\Big)^{3}=\frac{1}{\sigma_{\mathrm{ys}}^{\mathrm{t}}+\sigma_{\mathrm{ys}}^{\mathrm{c}}}\Big(\sigma_{\mathrm{ys}}^{\mathrm{t}}\sigma_{\mathrm{ys}}^{\mathrm{c}}+2\sigma_{\mathrm{pl}}^{z}\Big(\frac{l}{a_{\mathrm{s}}}\Big)^{2}\sin\beta(\sigma_{\mathrm{ys}}^{\mathrm{t}}-\sigma_{\mathrm{ys}}^{\mathrm{c}})-(2\sigma_{\mathrm{pl}}^{z}\Big(\frac{l}{a_{\mathrm{s}}}\Big)^{2}\sin\beta)^{2}\Big),\tag{9}$$

$$\pm\sqrt{2}\sigma_{\mathrm{pl}}^{x}\tan^{2}\beta\Big(\frac{l}{a_{\mathrm{s}}}\Big)^{3}=\frac{1}{\sigma_{\mathrm{ys}}^{\mathrm{t}}+\sigma_{\mathrm{ys}}^{\mathrm{c}}}\Big(\sigma_{\mathrm{ys}}^{\mathrm{t}}\sigma_{\mathrm{ys}}^{\mathrm{c}}+2\sigma_{\mathrm{pl}}^{x}\Big(\frac{l}{a_{\mathrm{s}}}\Big)^{2}\sin\beta(\sigma_{\mathrm{ys}}^{\mathrm{t}}-\sigma_{\mathrm{ys}}^{\mathrm{c}})-\Big(2\sigma_{\mathrm{pl}}^{x}\Big(\frac{l}{a_{\mathrm{s}}}\Big)^{2}\sin\beta\Big)^{2}\Big).\tag{10}$$

Similarly, for the equilateral triangular and circular cross sections in Fig. 5, the side length and diameter are denoted by a_{t} and a_{c}, respectively. Then, the depths of the neutral axis ζ_{t} and ζ_{c} can also be given by equating the forces above and below the neutral axis, i.e.,

$$\zeta_{\mathrm{t}}=\frac{\sqrt{3}}{2}a_{\mathrm{t}}\Big(\frac{\sigma_{\mathrm{ys}}^{\mathrm{c}}+\sigma_{\mathrm{a}}}{\sigma_{\mathrm{ys}}^{\mathrm{c}}+\sigma_{\mathrm{ys}}^{\mathrm{t}}}\Big)^{\frac{1}{2}},\tag{11}$$

$$\arcsin\Big(\frac{2\zeta_{\mathrm{c}}}{a_{\mathrm{c}}}\Big)+\frac{2\zeta_{\mathrm{c}}}{a_{\mathrm{c}}}\sqrt{1-\Big(\frac{2\zeta_{\mathrm{c}}}{a_{\mathrm{c}}}\Big)^{2}}=\frac{\pi}{\sigma_{\mathrm{ys}}^{\mathrm{c}}+\sigma_{\mathrm{ys}}^{\mathrm{t}}}\Big(\sigma_{\mathrm{a}}-\frac{\sigma_{\mathrm{ys}}^{\mathrm{t}}-\sigma_{\mathrm{ys}}^{\mathrm{c}}}{2}\Big).\tag{12}$$

The corresponding plastic moments of equilateral triangle and circular sections are then given by the integration $\int_{A}y\sigma\mathrm{d}A$, i.e.,

$$M_{\mathrm{p}}^{\mathrm{t}}=\frac{a_{\mathrm{t}}^{3}}{4}(\sigma_{\mathrm{ys}}^{\mathrm{c}}+\sigma_{\mathrm{a}})\Big(1-\sqrt{\frac{\sigma_{\mathrm{ys}}^{\mathrm{c}}+\sigma_{\mathrm{a}}}{\sigma_{\mathrm{ys}}^{\mathrm{c}}+\sigma_{\mathrm{ys}}^{\mathrm{t}}}}\Big),\tag{13}$$

$$M_{\mathrm{p}}^{\mathrm{c}}=\frac{1}{12}a_{\mathrm{c}}^{3}(\sigma_{\mathrm{ys}}^{\mathrm{c}}+\sigma_{\mathrm{ys}}^{\mathrm{t}})\Big(1-\Big(\frac{2\zeta_{\mathrm{c}}}{a_{\mathrm{c}}}\Big)^{2}\Big)^{\frac{3}{2}}.\tag{14}$$

In addition, the factor n is defined as the ratio of compressive and tensile strengths of the solid material, i.e.,

$$n=\sigma_{\mathrm{ys}}^{\mathrm{c}}/\sigma_{\mathrm{ys}}^{\mathrm{t}}.\tag{15}$$

3 Results and discussion

3.1 Effects of strut geometry

The uniaxial strength asymmetries of open-cell foams with different strut cross sections are numerically evaluated, as shown in Fig. 6. Ford and Gibson[8] concluded that two conditions lead to strength asymmetry, i.e., the solid material with different compressive and tensile strengths and the inclined struts loaded simultaneously by axial forces and bending moment. However, the results in Fig. 6 clearly show that even if there is no strength asymmetry (i.e., $n=1$) in the solid material, the open-cell foams with asymmetrical sectional struts (i.e., equilateral triangle) still exhibit an obvious strength asymmetry, which increases with increasing the relative density. When the relative density approaches 0.1, this value of strength asymmetry is about 1.063, which is in close agreement with the value of 1.04 obtained by analyzing yield surface based on a simple cubic unit cell[9]. As n becomes larger, each strength asymmetry of open-cell foams with different cross sections increases. The results illustrate that the asymmetrical section has the highest degree of strength asymmetry, while the circular section has the lowest one. In addition, the difference between the results of two symmetrical sections (i.e., square and circular sections) is slight, but it increases with increasing the relative density.

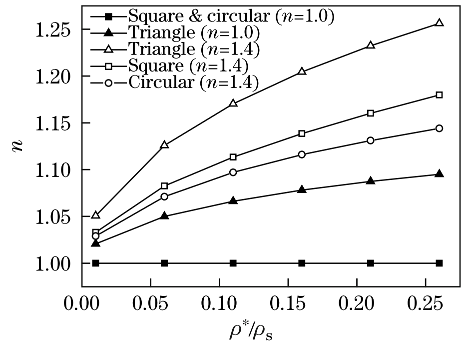

Fig. 6 Uniaxial strength asymmetry of open-cell foams with different cross sections

3.2 Effects of cell morphology

To describe the effects of cell morphologic anisotropy on strength asymmetry, the normalized strength, which is normalized by the strength of the solid material, is introduced into the following analysis. Figure 7 shows the normalized compressive strength in rise and transverse directions, which is the function of the relative density, with the anisotropic ratio varying from 1 to 1.6. The normalized tensile strength has the same trend with the compressive strength. The factor n is assumed to be 1.4, which is observed in many materials[8]. Considering the feasibility to perform the comparison with other existing results, the square cross section is adopted in this analysis. The open-cell foams with the other two cross sections can be easily demonstrated to have the similar tendency to that of square section with the same method.

In Figs. 7 and 8, the elongated Kelvin model predicates an increase in absolute values and asymmetry of strengths when the relative density increases. With a given relative density, the anisotropic open-cell foams have higher absolute normalized strengths than the isotropic ones, while it includes a higher degree of strength asymmetry in the rise direction than in the transverse direction. Moreover, the increase in the anisotropy causes an increase in the uniaxial strength as well as strength asymmetry in the rise direction. However, the trend is reversed in the transverse direction. When both the strength asymmetry of solid material and the anisotropic ratio reduce to unity, the normalized strengths can be reduced to the results of the simple Kelvin model. Then, the reduced results are compared with Gibson and Ashby's results. Using experimental data of the plastic collapse strength of foams, Gibson and Ashby concluded that $\sigma^*_{\rm pl}/\sigma_{\rm ys} \approx 0.3(\rho^*/\rho_{\rm s})^{3/2}$ for open cells, and $\sigma^*_{\rm pl}/\sigma_{\rm ys} \approx 0.23(\rho^*/\rho_{\rm s})^{3/2}(1+(\rho^*/\rho_{\rm s})^{1/2})$

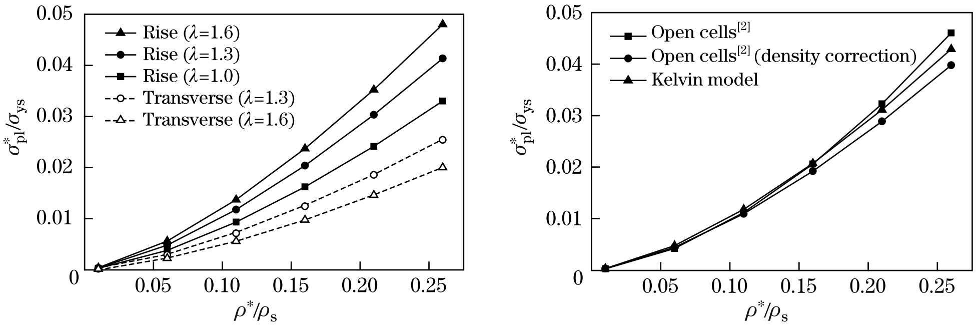

(a) For different anisotropic ratios (n=1.4)

(b) Comparison with Gibson's theoretical results (n=1 and λ=1)

Fig. 7 Normalized compressive strength of open-cell foams versus relative density including the density correction[1]. The results based on the Kelvin model are between the above two curves shown in Fig. 7(b), which demonstrates validity of the Kelvin model in predicting the strengths of open-cell foams.

The increase in the anisotropic ratio has a significant effect on the strength asymmetry of open-cell foams. The predicted curves in Fig. 8 show that as the anisotropic ratio increases, the strength asymmetry increases in the rise direction, while it decreases in the transverse direction. It may be the reduced axial force, one indispensable condition for the asymmetry, that weakens the effect of strength asymmetry of open-cell foams. The comparison in Fig. 8 also indicates that the factor, which has the largest effect on the predicted strength asymmetry of foams, is the ratio of the compressive to tensile yield strengths of solid material. In addition, the numerical results indicate that the ratio of plastic collapse strengths in the rise and transverse directions of open-cell foams is almost independent of the relative density. In Fig. 9, as n increases, this ratio for compressive strengths increases slightly, while it decreases slightly for tensile strengths, which verifies that the ratio of plastic collapse strengths in two directions is mainly determined by the cell anisotropy rather than the properties of solid material. Gibson and Ashby[1] derived the plastic collapse ratio based on the anisotropic cubic unit cell,

$$\frac{(\sigma^*_{\mathrm{pl}})_3}{(\sigma^*_{\mathrm{pl}})_1} = \frac{2R}{1 + 1/R}, \tag{16}$$

where R is the ratio of the longest dimension to the shortest one of the cubic cell.

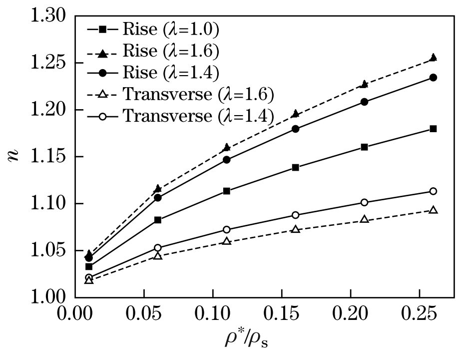

Fig. 8 Uniaxial strength asymmetry in rise and transverse directions of anisotropic open-cell foams ($n = 1.4$)

As shown in Fig. 9, when the anisotropic ratio is small ($\lambda \leqslant 1.3$), the predicted curve (when $n = 1$) of the elongated Kelvin model is much closer to the experimental data than that of the anisotropic cubic model. However, as the anisotropic ratio increases, the Kelvin model overestimates the ratio, while the Gibson's cubic model underestimates it. The average results of such two models agree very well with the experimental data. The discrepancy between theoretical models and experimental data may be due to that these regular models do not consider the natural variability observed in realistic open-cell foams, where the non-periodic cells are more general[8]. However, the ignored consideration of strut geometry and cell morphology of testing samples can effectively explain the dispersity of experimental data.

4 Conclusions

The way how the uniaxial strength asymmetry in anisotropic open-cell foams depends on the relative density, the cell morphology, the strut geometry, and the properties of solid material is studied. By introducing different compressive and tensile strengths of the solid material into

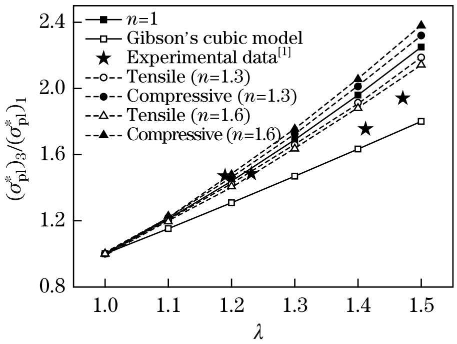

Fig. 9 Ratio of plastic collapse strengths in two directions for both tension and compression plotted against anisotropic ratio of different models and experimental results

the elongated Kelvin model, this paper confirms that the density-dependent uniaxial strength asymmetry of the open-cell foams can arise not only when the solid material has a difference between compressive and tensile strengths but also when the strut cross section has an asymmetric shape. The results of square, equilateral triangle, and circular cross sections are compared. The open-cell foams with equilateral triangle section are found to have a much greater degree of strength asymmetry than that of square and circular ones, and the results of the circular section are the lowest. These conclusions illustrate the importance of consideration of strut geometry in successful prediction of the strength of the open-cell foams. In addition, the increasing anisotropic ratio of open-cell foam can result in an increase in the absolute strength as well as the strength asymmetry in the rise direction but a decrease in the transverse direction. The plastic collapse ratio of two directions is verified to depend mainly on the cell geometric anisotropy. To confirm the Kelvin model's ability to describe the general behaviors of the realistic open-cell foams, the predicted results are compared with Gibson and Ashby's results as well as the experimental data of tensile and compressive strengths reported in the literature. These comparisons indicate that the elongated Kelvin model is valid to explain the strength asymmetry presented in the realistic open-cell foams. Given that this analysis is limited to the uniaxial loading of anisotropic open-cell foams, the failure behaviors under the multiaxial loading need a further research.

References

[1] Gibson, L. J. and Ashby, M. F. *Cellular Solids: Structure & Properties*, Pergamon Press, Oxford (1997)

[2] Gibson, L. J., Ashby, M. F., Zhang, J., and Triantafillou, T. C. Failure surfaces for cellular materials under multiaxial loads I: modeling. *International Journal of Mechanical Sciences*, **31**(9), 635–663 (1989)

[3] Gioux, G., McCormack, T. M., and Gibson, L. J. Failure of aluminum foams under multiaxial loads. *International Journal of Mechanical Sciences*, **42**(6), 1097–1117 (2000)

[4] Kim, H. S. and Al-Hassani, S. T. S. The effect of doubly tapered strut morphology on the plastic-yield surface of cellular materials. *International Journal of Mechanical Sciences*, **44**(8), 1559–1581 (2002)

[5] Amsterdam, E., Hosson, J. D., and Onck, P. R. On the plastic collapse stress of open-cell aluminum foam. *Scripta Materialia*, **59**(6), 653–656 (2008)

[6] Marchi, C. S. and Mortensen, A. Deformation of open-cell aluminum foam. *Acta Materialia*, **49**(19), 3959–3969 (2001)

[7] Despois, F. J., Mueller, R., and Mortensen, A. Uniaxial deformation of microcellular metals. *Acta Materialia*, **54**(16), 4129–4142 (2006)

[8] Ford, C. M. and Gibson, L. J. Uniaxial strength asymmetry in cellular materials: an analytical model. *International Journal of Mechanical Sciences*, **40**(6), 521–531 (1998)

[9] Xie, L. S. and Chan, K. C. The effect of strut geometry on the yielding behaviour of open-cell foams. *International Journal of Mechanical Sciences*, **48**(3), 249–255 (2006)

[10] Perrot, C., Panneton, R., and Olny, X. Periodic unit cell reconstruction of porous media: application to open-cell aluminum foams. *Journal of Applied Physics*, **101**(11), 113538 (2007) DOI 10.1063/1.2745095

[11] Jang, W. Y., Kraynik, A. M., and Kyriakides, S. On the microstructure of open-cell foams and its effect on elastic properties. *International Journal of Solids and Structures*, **45**(7), 1845–1875 (2008)

[12] Gong, L., Kyriakides, S., and Jang, W. Y. Compressive response of open-cell foams, part I: morphology and elastic properties. *International Journal of Solids and Structures*, **42**(5), 1355–1379 (2005)

[13] Xie, L. S., Tong, G. Q., and Gao, L. Elastic properties of the Kelvin foams with open-cells. *Chinese Journal of Applied Mechanics*, **24**(1), 75–79 (2007)

[14] Thiyagasundaram, P., Sankar, B. V., and Arakere, N. K. Elastic properties of open-cell foams with tetrakaidecahedral cells using finite element analysis. *AIAA Journal*, **48**(4), 818–828 (2010)

[15] Jang, W. Y., Kyriakides, S., and Kraynik, A. M. On the compressive strength of open-cell metal foams with Kelvin and random cell structures. *International Journal of Solids and Structures*, **47**(21), 2872–2883 (2010)

[16] Li, Z. Q., Xi, C. Q., Jing, L., Wang, Z. H., and Zhao, L. M. Effect of loading rate on the compressive properties of open-cell metal foams. *Materials Science and Engineering A*, **592**(13), 221–229 (2014)

[17] Xu, W. G., Zhang, H. T., Wei, W., Yang, Z. M., and Zhang, J. S. Numerical and experimental investigations on the electrical conductivity of foam materials. *Special Topics & Reviews in Porous Media: An International Journal*, **2**(1), 35–42 (2011)

[18] Yang, X. H., Kuang, J. J., Lu, T. J., Han, F. S., and Kim, T. A simplistic analytical unit cell based model for the effective thermal conductivity of high porosity open-cell metal foams. *Journal of Physics D: Applied Physics*, **46**(25), 255302 (2013)

[19] Lu, Z. X., Zhang, C. G., Liu, Q., and Yang, Z. Y. Surface effects on the mechanical properties of nanoporous materials. *Journal of Physics D: Applied Physics*, **44**(39), 395–404 (2011) DOI 10.1088/0022-3727/44/39/395404

[20] Lu, Z. X., Liu, Q., and Huang, J. X. Analysis of defects on the compressive behaviors of open-cell metal foams through models using the FEM. *Materials Science and Engineering A*, **530**, 285–296 (2011)

[21] Lu, Z. X., Huang, J. X., and Chen, X. Analysis and simulation of high strain compression of anisotropic open-cell elastic foams. *Science China Technological Sciences*, **53**(3), 863–869 (2010)

[22] Lu, Z. X., Liu, Q., and Chen, X. Analysis and simulation for the tensile behavior of anisotropic open-cell elastic foams. *Applied Mathematics and Mechanics (English Edition)*, **35**(11), 1437–1446 (2014) DOI 10.1007/s10483-014-1874-7

[23] Sullivan, R. M., Ghoson, L. J., and Lerch, B. A. A general tetrakaidecahedron model for open-celled foams. *International Journal of Solids and Structures*, **45**(6), 1754–1765 (2008)

[24] Zhu, H. X., Knott, J. F., and Mills, N. J. Analysis of the elastic properties of open-cell foams with tetrakaidecahedral cells. *Journal of the Mechanics and Physics of Solids*, **45**(3), 319–343 (1997)